29th Congress of the International Council of the Aeronautical Sciences
St. Petersburg, Russia; September 7-12, 2014

NEW CHALLENGES FOR ENGINE NACELLE COMPARTMENTS PRESSURE AND THERMAL LOADS MANAGEMENT WITH AIRCRAFT ENGINE EVOLUTION

Olivier Verseux ; Yannick Sommerer
AIRBUS OPERATION S.A.S.,
316 Route de Bayonne, 31060 Toulouse Cedex 03, France,

Keywords: *aircraft engine compartments, pressure & thermal loads*

Abstract

The improvement of civil aircraft engine performances, consumption and acoustic signature lead the engine manufacturers to increase both the by-pass ratio (BPR) and the overall pressure ration (OPR) respectively defined as the ratio of the engine secondary flux mass flow rate to the primary flux mass flow rate and the ratio of the pressure at the exit of the engine compressor to the ambient pressure. Those trends impact the engine to aircraft integration work through technical evolutions such as changes of the geometrical characteristics with larger fans, the use of new casing or cowling materials and warmer engine cores. It particularly affects the engine nacelle zones regarding the thermal environment for the mounted system items and the pressure loads on nacelle structures.

The purpose of this paper is to identify and analyze technical risks for nacelle ventilation and propulsion system items thermal integration.

The rise of the BPR induces a decrease of the engine secondary flow pressure also called fan pressure ratio (FPR) and thus degrades the engine core compartment ventilation major source.

The increase of OPR allowed by the use of new materials (alloys, ceramics) and core internal cooling technologies involves engine primary flow temperature and pressure rise.

On one hand, the combined effect of a loss of nacelle cooling performances and higher heat sources generates a more stringent thermal environment for the system items and structures located in the nacelle core compartment. On the other hand the increase of primary flux pressures constraints more and more the nacelle design to keep on mastering the effects of an air duct rupture as required by the certification.

Those trends are already experimented by Airbus through neo program where a more particular attention has been paid to the nacelle cooling and the alleviation of air duct rupture consequences.

1 Introduction

The engine compartment cooling and overpressure relief system previously seen as secondary key design factors from a propulsion system (defined as engine, nacelle, pylon and all mounted system items) integration stand point have become throughout the last Aircraft developments a major technical items impacting the global design. It is now to be considered in the early phase of a propulsion system development to avoid facing issues during conception and verification phases.

1.1 Engine compartment ventilation description and stakes

The engine compartments are delimited by the engine casing and the nacelle cowling. Those compartments are usually defined as fire zones or flammable fluid leakage zones. As a

consequence a specific sealing of these zones is to be designed and fire prevention guaranteed by the fire extinguishing system for fire zones are to be implemented. Those compartments contain equipment items which need to be maintained in an acceptable environment ensuring the safety and the reliability for the aircraft.

A cooling of those compartments is then necessary to cope with fire requirements and equipment items temperature limits.

The cooling is realized by a dynamic inlet scoops (NACA type) picking up air from the free stream when the compartment outer cowl is surrounded by outside air. This category encompasses the fan compartment also called zone 1 colored in green and the grey zone of an open rotor as depicted in Fig. 1.

For the compartments located between the engine primary and secondary fluxes, cooling air is bled from the secondary flow through holes drilled in the cowling thanks to a pressure differential between the secondary flow and the compartment. The depressurization of the compartment with regards to the engine secondary flow is generated by a ventilation outlet located at a low pressure area which is usually close to the free stream pressure. The cooled air is distributed in the zone through either a manifold or local simple ventilation holes in the cowling. The main concerned area is the blue zones of Fig. 1 called core compartment or zone 3.

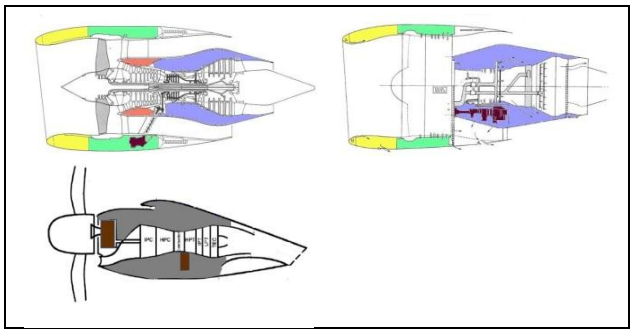

Fig. 1: Nacelle engine compartments for various engine configurations – colored zones

The design of the ventilation is driven by the certification requirements of CS.25 / JAR.25 but also by the performance impacts on engine and aircraft.

The present article **focuses on zone 3** as it is the hottest compartment and usually the most congested area with numerous installed systems especially when the engine is a core mounted gearbox one. Only the turbofan engines are addressed, but conclusions may be derived to turboprop engines for particular aspects.

1.2 Engine compartment pressure relief system

The certification paragraph CS 25.1103(d) of [4] specifies that a duct rupture shall not lead to an aircraft hazardous condition. The compliance is done by showing that a full rupture of the high pressure air bleed duct does not overstress the structures and does not induce uncontrolled system behaviour.

To relieve the over pressure in a nacelle compartment consecutive to an air duct rupture, a pressure relief system is installed. It usually consists in a latched door that is triggered open under a given pressure differential and discharging air outside the compartment. It allows reducing, first the pressure peak occurring few hundredth seconds after the burst and secondly the stabilized pressure seen by the IFS (Nacelle thrust reverser inner fixe structure).

It may be necessary to alleviate the over-temperatures in a compartment consecutive to a duct rupture event. In this case, a temperature detection system is implemented. Once triggered this system either commands the closure of valves associated to the air rupture source or sends a cockpit warning.

As for the compartment cooling and for the same reasons, the air duct rupture consequences in the core compartment only are addressed.

2 Engine evolution trends

In order to improve civil aircraft engine performances, consumption and acoustic signature, the engine manufacturers develop engines with larger fans and higher compressed core flow. The thrust is mainly produced by a low pressurized massive fan flow and the optimized thermodynamic cycle of the core flow produces torque powering the fan with an increased efficiency. The geared turbofan

perfectly illustrates this trend. As a consequence both BPR and OPR are being increasing.

Those engine evolutions impact the propulsion system and its integration to aircraft. It affects in particular the thermal and pressure loads considered for the engine nacelle compartment system and structural design. The rise of the BPR induces a decrease of the engine secondary flow pressure also called fan pressure ratio (FPR) and thus degrades the engine core compartment ventilation major source.

The increase of OPR allowed by the use of new materials (alloys, ceramics) and core internal cooling technologies involves engine primary flow temperature and pressure rise.

On one hand, the combined effect of a loss of nacelle cooling performances and higher heat sources generates a more stringent thermal environment for the system items and structures located in the nacelle core compartment. On the other hand the increase of primary flux pressure constraints more and more the nacelle design to keep on mastering the effects of an air duct rupture as required by the certification.

Those trends are already experimented by Airbus through neo program where a more particular attention has been paid to the nacelle cooling and the alleviation of air duct rupture consequences.

Other challenges not addressed in this paper such as the rise of heat to be dissipated by the engine trough the fluids (oil, fuel and air) is also a major point especially for the geared turbofan.

Paragraphs 2.1 and 2.2 quantify FPR and OPR trends to feed case studies on system item thermal integration impact and nacelle pressure load impact assessments developed in paragraph 3.

2.1 FPR reduction

Fig. 2 plots FPR of engines installed on Airbus aircraft during the last 20 years and projected towards the 15 coming years. EIS means entry into service. As the purpose of this exercise is to simply extract a trend, engines from 22000 to 70000 pound thrust are mixed. The figures for the future engines are preliminary estimates coming from exchanges with engine manufacturers.

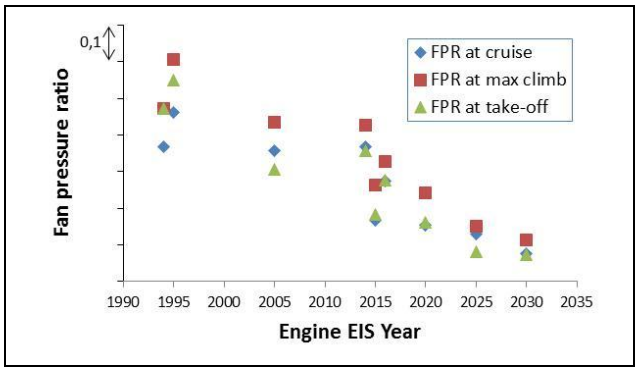

Fig. 2 : FPR versus Engine EIS Year (Airbus Fleet)

A FPR diminution of roughly 25% is observed from late Nineties to 2030.

2.2 OPR rise

OPR are plotted in Fig. 3 among the same sample of engines as for FPR.

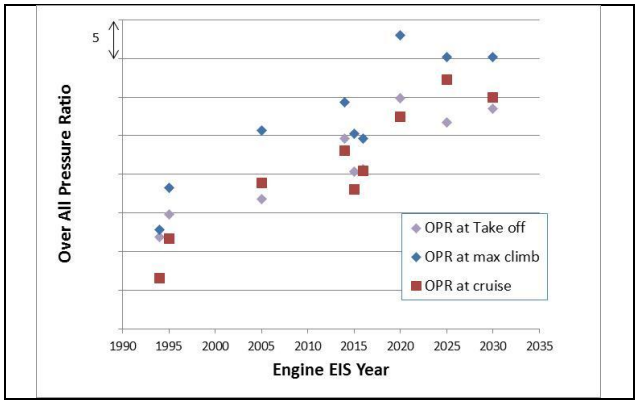

Fig. 3 : OPR versus engine EIS year

The consequences of the OPR increase on engine core flow temperature are plotted in Fig. 4. T_3 defined as the engine core flow air temperature at compressor exit and T_{LPT} (also called T49) as the engine core gas temperature at low pressure turbine inlet are referent points for core engine casing temperatures and thus to assess the impact on core compartment temperatures. The linear extrapolation proposed in Fig. 4 are just plotted to highlight a general trend and not to depict the evolution of the concerned temperature as a linear over the years.

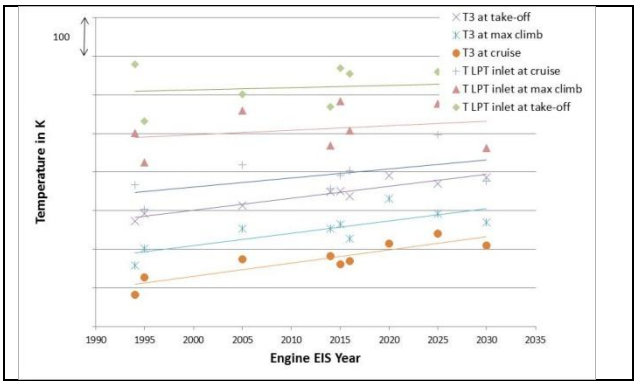

Fig. 4: Primary flux temperatures versus engine EIS year

T_3 increases by 100°C from 1995 to 2030. This trend is obviously not linear and will depend on the technology adopted by the engine manufacturers to design their engines.

T_{49} plots show a global slight increase at Take-off condition whereas the increase is more pronounced in cruise conditions. It is to be noted that due to the mixing of different engine technologies and thrust ranges the scattering between engines is large throughout the years.

3 Impact on core compartment thermal and pressure loads

In order to illustrate the consequences of the FPR and OPR evolutions on propulsion system integration, 2 exercises have been led and presented hereafter.

3.1 Consequence on system items thermal integration

The purpose is to estimate the temperature evolution of a system item located in a core compartment versus different engines characterized by a couple FPR - OPR.

Ventilation cooling performance

First of all, the ventilation cooling performance is studied through the evaluation of the HTC (convective Heat Transfer Coefficient).

Convective heat transfer coefficients have been estimated for a ventilation jet, generated by FPR through a 2.54cm diameter hole drilled in the nacelle cowling, impacting a system located 10cm downstream the jet inlet for different engine FPR.

The following assumptions and inputs have been considered:

- Mass flow rates through ventilation hole are calculated thanks to discharge coefficients of [1];
- The core compartment pressure is 0,5 psi above outside static pressure, figure roughly targeted to obtained some thrust recovery from the air exiting the core compartment;
- Heat transfer coefficients are based on [2], [3] and Airbus internal references;
- Re, Pr and Nu numbers are calculated at secondary air flow static temperature T_{13};
- The impacted wall is considered isotherm.

The exercise is performed with similar engines range of thrust mounted on Airbus Single aisle Aircraft for a BPR varying in a range of 6 to 15. HTC is given at stagnation point and at r = 2,5*Dhole away from the stagnation point for different engines identified via their FPR. (Dhole: ventilation hole diameter)

FPR	1,57	1,475	1,367	1,33
ventil mass flow g/s	39,5	39	36	35
h stagnation W/m²K	350	345	337	330
h W/m²K at r/Dhole=2,5	181	179	169	165

Tab. 1: HTC in cruise conditions 35000 ft

FPR	1,67	1,477	1,38	1,28
ventil mass flow g/s	99	86	70	57
h stagnation W/m²K	641	589	523	460
h W/m²K at r/Dhole=2,5	359	324	280	240

Tab. 2 : HTC in take-off conditions at SL/ Mn0.25/ ISA+15°C

The reduction of the cooling effect generated by the decrease of FPR is obvious. Then solutions to recover an equivalent cooling performance of a FPR=1,38 engine to a FPR=1,67 one have been tested. The purpose is to keep the legacy ventilation architecture and to play with the hole sizes and types from [1] as presented in Tab. 3. All other inputs are the same and the exercise is achieved at take-off condition since it is usually the most constraining phase for thermal integration. The results are encompassed in Tab. 4.

Vent hole type	description	Nomenclature
Straight Dhole=25mm	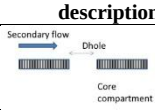	Basic 25
Oblique Dhole=25mm	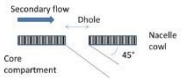	Oblic 25
Straight Dhole=30mm	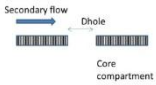	Basic 30
Oblique Dhole=30mm	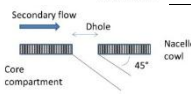	Oblic 30
Dynamic hole Dhole=30mm	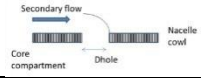	Dyn 30

Tab. 3 : Ventilation hole description

ventilation hole type	basic 25	basic 25	oblic 25	basic 30	oblic 30	dyn 25
FPR	1,67	1,38	1,38	1,38	1,38	1,38
ventil mass flow g/s	99	70	80	100	115	106
h stagnation W/m²K	641	523	562	490	530	662
h W/m²K at r/Dhole=2,5	359	280	307	272	300	377

Tab. 4 : cooling efficiency in take-off conditions at SL/ Mn0.25/ ISA+15°C for various vent hole types

Tab. 4 shows that the recovery of the ventilation mass flow rate by hole enlargement is not sufficient to ensure an equivalent cooling performance. Actually the reduction of the FPR induces a decrease of ventilation jet velocity and thus a decrease of heat transfer coefficient value. The only way to ensure roughly the same cooling effect is to recover some dynamic pressure thanks to a dynamic scoop. But this protruding device into the fan flow is not acceptable since it impacts the engine specific fuel consumption (SFC) too significantly. It is necessary to rework the inlet shape to optimize its performances taking into account the constraint such as the minimization of its footprint impact on the acoustic surface and stress impact. Currently, optimized oblique simple holes (inlet shapes smoothed compared to presented one in Tab. 3) are privileged as an acceptable compromise.

The same calculation is achieved with a lower pressure ratio. Tab. 5 shows that even with a dynamic scoop it is not possible to recover the same cooling effect as the one produced with FPR=1,67 engine.

ventilation hole type	basic 25	basic 25	dyn 25	dyn 25
FPR	1,67	1,48	1,38	1,28
ventil mass flow g/s	99	86	106	86
h stagnation W/m²K	641	589	662	584
h W/m²K at r/Dhole=2,5	359	324	377	323

Tab. 5 : Heat transfer coefficients for different FPR in take-off conditions at SL/ Mn0.25/ ISA+15°C

System temperature estimate

The present study considers a system installed in a core compartment in the neighbourhood of the high compressor engine casing. It exchanges heat by radiation (Q_{rad}) with the engine on its lower surface and ventilation jet at T_{13} (Fan flow air temperature) impacts its upper surface. Q_{conv} is the heat exchange by convection. Fig. 6 describes the model assumptions. Upper and lower surfaces (S) are circular with a diameter of 10cm. The system also dissipates some internal heat (P_{dissip}). The reference engine is from end of the Nineties and the projection is done on 2025 EIS engine. Both engines have the same range of thrust and are mounted on the same aircraft type.

The system is considered at a uniform temperature (lumped mass, Biot Number less than 0,1). The view factor between the system lower surface toward the engine casing is 1. The considered engine casing part is at T_3. The heat exchange coefficient (h_{aver}) is an averaged value over the surface of the HTC distribution presented in Fig. 5 which presents HTC profiles calculated for different ventilation hole types and various FPR. Those profiles are extracted from Airbus internal correlation mixing experimental and numerical databases and ensure a conservative assumption for thermal integration work.

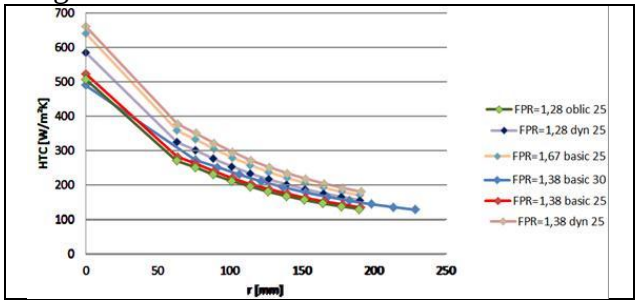

Fig. 5 : HTC profiles (HTC vs distance to stagnation point) for various hole configuration and FPR in take-off conditions at SL/ Mn0.25/ ISA+15°C

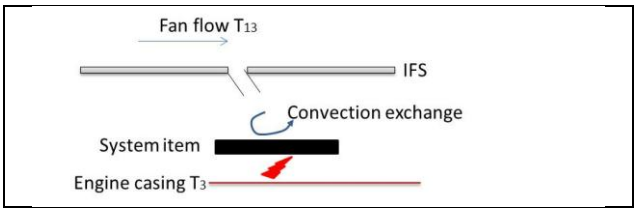

Fig. 6 : model description

The reference engine has basic ventilation design (thin holes drilled into the IFS). The projected engine has ventilation ensured by oblique ventilation holes flowing fan air at T_{13} upon the system item.

Writing enthalpy balance performed at system level:

$$P_{dissip} + Q_{conv} + Q_{ray} = 0$$

$$Q_{conv} = -h_{aver} S (T - T_{13})$$

$$Q_{ray} = \frac{-\sigma (T^4 - T_3^4)}{\frac{1-\epsilon}{\epsilon S} + \frac{1}{S} + \frac{1-\epsilon_3}{\epsilon_3 S_3}}$$

Results collected in Tab. 6 are obtained by solving the previous equation system in *T* which is the system item temperature.

	ventil hole	P_{dissip} W	T_3 °C	T_{13} °C	h_{aver} W/m²K	T °C
ref engine	basic 25	0	T_3 ref	T_{13} ref	476	135
2025 EIS engine	oblic 25	0	T_3 ref + 97	T_{13} ref - 31	367	149
ref engine	basic 25	250	T_3 ref	T_{13} ref	476	199
2025 EIS engine	oblic 25	250	T_3 ref + 97	T_{13} ref - 31	367	233

Tab. 6 : System temperature vs engine EIS year

It results a significant increase of system average temperature with direct consequences on material choice, system architecture or location.

For instance, taking Tab. 6 results for a non-dissipating system which could be either a structural part or a system crossed by oil, the use of epoxy composite material is compromised for the structural one and relocation is necessary for the second one. As a second example, the use of aluminium for dissipating system is risky, knowing that the actual temperature is barely uniform and some hot spots exist. Locally, more than 50°C of exceedance with regards to the average temperature has been already experienced.

3.2 Pressure load on nacelle structures

Among the load cases accounted to size the nacelle IFS, the duct burst case impact is to be analysed with regards to the engine evolution. The usual sizing case is a burst simulated at highest engine compressor bleed port.

The burst mass flow rate is a shock flow injected in the core compartment. It is expressed as:

$$Q_{burst} = F . {P_3}/{\sqrt{T_3}} \quad (1)$$

F is a constant flow function dependent of the efficient section of shock plate and P_3 the pressure at high pressure compressor exit.

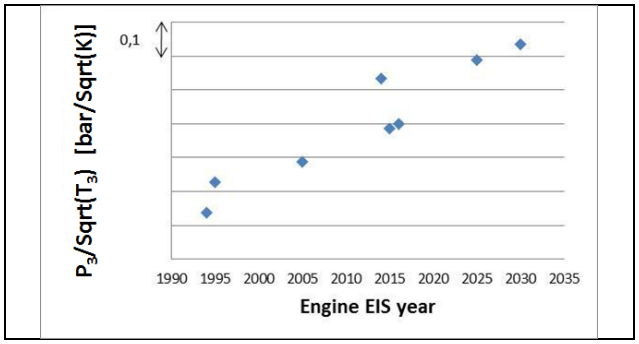

Fig. 7 : $P_3/Sqrt(T_3)$ versus engine EIS year

Fig. 7 shows an increase of the ratio $P_3/Sqrt(T_3)$ and thus an increase of Q_{burst} and thus internal core compartment pressure at a given geometrical configuration in case of burst event. In the same time the FPR decreases as shown in Fig. 2, directly leading to a decrease of the counter-pressure exerted on the external skin of the IFS. It results that the load applied on the IFS in case of air duct rupture in the core compartment will theoretically continue increasing with the next engine generations.

The assessment of the evolution of the resultant delta pressure on the IFS is not straight forward. Nevertheless, the following exercise tries to quantify it.

On the external surface of the IFS the diminution of the pressure can be directly deduced from the diminution of the FPR. It is not totally true as the pressure of interest is the secondary flow static pressure at the IFS outer surface which the profile depends on geometrical characteristics of the fan blades and secondary flow channel. But the trend is

considered correct and will be extracted from Fig. 2.

The assessment of evolution of the pressure exerted on the internal IFS structure in case of air duct rupture is trickier. A method is proposed hereafter.

In stabilized conditions, the burst mass flow rate is discharged outside the core compartment through different surfaces such as drain holes, core compartment ventilation exit and pressure relief door. Considering an isentropic flow:

$$Q_{burst} = \frac{P_i}{\sqrt{T_i}} S \sqrt{\frac{2\gamma}{r(\gamma-1)}} \sqrt{\left(\frac{P_e}{P_i}\right)^{2/\gamma}} \sqrt{\left[1-\left(\frac{P_e}{P_i}\right)^{(\gamma-1)/\gamma}\right]} \quad (2)$$

T_i and P_i are respectively the temperature and the pressure in the core compartment. T_e and P_e are the temperature and pressure at core compartment exits. S is the total efficient surface of the exits. The gas specific constant r is 287 $J \cdot kg^{-1} \cdot K^{-1}$ and compressibility coefficient γ is 1,4 for air.

In stabilized conditions the core compartment temperature T_i will be assumed at burst temperature T_3. The combination of (1) and (2) gives:

$$P_3 = K \frac{P_i}{P_e} \sqrt{\left(\frac{P_e}{P_i}\right)^{2/\gamma}} \sqrt{\left[1-\left(\frac{P_e}{P_i}\right)^{(\gamma-1)/\gamma}\right]} \quad (3)$$

With K constant:

$$K = \frac{1}{F} S P_e \sqrt{\frac{2\gamma}{r(\gamma-1)}} \quad (4)$$

For air bleed air burst at take-off condition which is usually the design case, the ratio P_e/P_i is within a range 0,55 to 0,85.

Setting $x=P_e/P_i$ and $a=(1-\gamma)/\gamma$, (3) becomes:

$$P_3 = K\sqrt{(x^a)^2 - x^a} \quad (5)$$

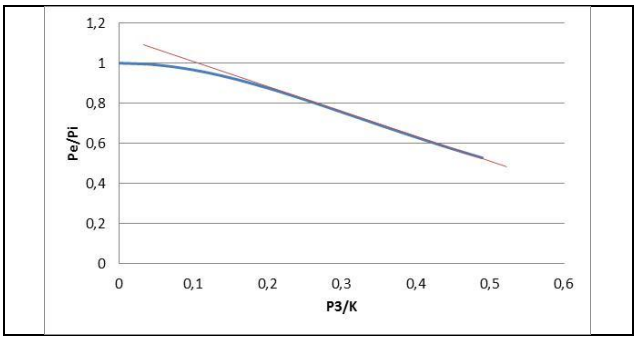

Fig. 8 : Plot of (5)

Fig. 8 shows a linear relationship between P_3 and $1/P_i$, K and P_e being constants.

In order to demonstrate this behaviour in the range of interest, Taylor's theorem to P_3/K at the second order around x_0 have been applied:

$$\frac{P_3(x)}{K} = \sqrt{(x_0{}^a)^2 - x_0{}^a} + A(x-x_0) + B(x-x_0)^2 + h_2(x)(x-x_0)^2 \quad (6)$$

where

$$A = \frac{1}{2\sqrt{(x_0{}^a)^2 - x_0{}^a}} (2a x_0{}^{2a-1} - a x_0{}^{a-1})$$

$$B = \frac{1}{4\sqrt{(x_0{}^a)^2 - x_0{}^a}} (2a(2a-1)x_0{}^{2a-2} - a(a-1)x_0{}^{a-2}) - \frac{1}{8}(x_0{}^{2a} - x_0{}^a)^{-3/2}(2a x_0{}^{2a-1} - a x_0{}^{a-1})^2$$

$$\lim_{x \to x_0} h_2(x) = 0$$

For x_0=0,7 A=-0,796 and B=0,107.

For a variation of 0,15 of x around x_0, the term $B(x-x_0)^2$ is roughly two hundredth of $A(x-x_0)$. The second order of the development is then neglected in the considered range [0,55;0,85] of x. It confirms the linear relationship observed between $1/P_i$ and P_3 in Fig. 8.

The assessment of the engine evolution impact on pressure exerted on the IFS is then proposed using the previous relation.

The reference engine is an existing engine and the stabilized pressure following an air duct rupture is extrapolated to an engine generation 10 years ahead. The propulsion systems are assumed to be in the same configuration (same shock plate at bleed port, same pressure relief system, same ventilation architecture and exit area).

For a delta P_3 of 0,675 bar between the 2 engines, the stabilized pressure P_i increase is 0,18 bar. In the same time the counter-pressure of the secondary flow decrease is 0,11 bar roughly. It results an increase of about 0,3 bar or 4,35 psia on the IFS of a nacelle mounted to a 2025 EIS engine, which is a significant stress impact on the structure.

Although the peak pressure evolution cannot be estimated (too much dependence on pressure relief system characteristics) this exercise shows that the engine evolution has a significant impact on the nacelle design. It is then necessary to engage fine trade-offs between structural strength and weight, size on the ventilation outlet and nacelle aerolines, pressure relief system and drag impact. But the improvement area is thin as the reference propulsion engine already takes benefit of fine tuning of here above parameters.

4 Conclusions and way-forward

The presented analyse shows that the engine evolution, illustrated by higher core flow compression and larger fan, induces additional stress on nacelle structural parts and make the propulsion system thermal integration trickier.

Several options are explored or already implemented by Airbus and their partners to anticipate and contain the observed trend on projected engines.

4.1 Processes, methods and tools

Considering the above conclusions, it is mandatory for the future engine developments to take into account pressure and thermal loads constrains earlier in the development phase. The objective is to anticipate integration issues and to be able to influence the design. At early phase, larger flexibility exists on design which allows performing trades and optimizing the architecture with reasonable constraints. However such optimisation or trade-off analysis is not an easy task as it requires:

- The development of specific modelling based on engineering knowledge on previous engines and extrapolation capabilities to future engines. Thermal pneumatic 0D models are often used for such studies but a rigorous simulation V&V process is required;
- An efficient concurrent work with engine and nacelle manufacturers to share relevant inputs. In parallel, a special attention must be paid on data management and traceability. Then a specific business workflow has to be agreed between all partners;
- A multi-objective optimization involving multi-physics models will be preferred to an optimization at component level.

In order to support efficiently the design phase, Airbus is developing specific tools for data management, business workflow and simulation workflow encompassed in an integrated simulation platform. It allows applying distributed calculation approach between stakeholders as presented in [5] in order to reduce the development margins while respecting the reliabilities, intellectual property and know-how of each partner.

Airbus short term objective is to widely extend the usage of this simulation platform to engine, nacelle and system manufacturers.

4.2 Margin reduction & sizing conditions

Covering a whole flight envelope as required by certification, leads to take numerous design margins to remove some uncertainties in particular those ones link to sizing cases definition. For instance, the worst flight condition cumulated to the worst equipment thermal state and worst engine thermal behaviour are considered for system thermal integration. However from a statistical point of view, the occurrence of such configuration is extremely remote. Then, for specific cases, a statistical approach may be considered to reduce the margins. Here again, the concurrent work with partners is key as a large data set is to be shared and managed. This is already successfully experienced by Airbus for some propulsion system aero-thermal integration works and tools are now operational to widely extend the application of such an approach.

4.3 High fidelity modelling

The reduction of the design margins and the optimization during the detailed design phase requires accurate modelling. Efforts have been made by Airbus for more than a decade to develop high fidelity modelling [6], [7] and [8] for engine nacelle compartments aero-thermal characterization. For such complex flows, unsteady 3D CFD modelling is required to get accurate predictions and confidence in the results. A special attention must be paid on grid refinement and turbulence modelling leading to models requiring thousands of CPU hours to be solved. Today, thanks to high performance computing deployed at Airbus (#1 of T500 industrial HPC in 2011; new HPC generation targeting the Petaflop; objective of Zettaflop in 2030), computational time is no longer an issue. The main challenge concerns the analysis lead time reduction. Then an accurate modeling is preferred in order to minimize engineers cost for results validation and rework.

Efforts have been also made to develop powerful tool to analyse test results and to extrapolate measured temperatures to the worst conditions. It relies on advanced identification models [9]-[10].

4.4 Ventilation technology and architecture

Active ventilation, such as electric and mechanical blowing or jet pump effect, is explored. Transportation of heat through heat pipes towards colder area to ease the cooling is also studied.

Alternative pressure relief systems are also developed with nacelle manufacturers.

Those activities are usually carried on through research and technology projects in collaboration with several partners. It is necessary to further develop those projects to master the future propulsion system integration challenges described in the present paper.

4.5 System protection and adaptation

At early design phases of an Aircraft program, thermal integration is dealt with the system manufacturers. It may lead to system redesign in order to better control the internal thermal dissipation or to reorganize the internal conductive paths. Re-localisation, addition of thermal or radiative protections are also considered. Nevertheless, those technical solutions are limited and it is today necessary to envisage and develop alternative solutions.

References

[1] Vedeshkin G, Dubovitskiy A, Bondarenko B, Verseux O. Experimental investigations of hydraulic devices performance in aviation engine compartment. *ICAS 2012, 28th International congress of the aeronautical sciences*.

[2] Jambunathan K, Lai E, Moss M, Button B. A review of heat transfer data for single circular jet impingement. *Int. J. Heat and Fluid Flow*, Vol. 13, No. 2, June 1992.

[3] Rohsenow W, Hartnett J, Cho Y. *Handbook of heat transfer*. Third edition, McGraw-Hill, 1998.

[4] European Aviation Safety Agency. *Certification Specifications and Acceptable Means of Compliance for Large Aeroplanes CS-25 Amendment 14*. 19 December 2013

[5] Sommerer Y, Nguyen Q.H, Dubourg G. *Collaborative engineering by multi-partner distributed simulation for powerplant thermal integration.* NAFEMS 2013, 1st SPDM Conference, Salzburg 09-12 June 2013.

[6] Boileau M, Duchaine F,. Jouhaud J.-C, and Sommerer Y. *Large Eddy Simulation of heat transfer around a square cylinder using unstructured grids*. AIAA Journal, Vol.51, No. 2 (2013), pp. 372-385.

[7] Sommerer Y, Couton D, Plourde F. *Dissipative equipment thermal integration in turbo-engine nacelle compartment: experimental and numerical evaluation of heat transfer coefficient*. ASME Turbo Expo - June 16-20, 2014, Düsseldorf.

[8] Dauptain A, Cuenot B, and Gicquel L.Y.M. *Large Eddy Simulation of a stable supersonic jet impinging on a flat plate*. AIAA Journal, 48(10):2325-2338, 2010. jx

[9] Uriz Jauregui F, Remy B, Degiovanni A, Verseux O. *Improved temperature extrapolation methods for powerplant systems*. AIAA-ASME congress, June 2010

[10] Uriz Jauregui F, Remy B, Degiovanni A, Verseux O. *Model identification for temperature extrapolation in aircraft powerplant systems*. International Journal of Thermal Sciences, Vol. 64 (February 2013), pp. 162-177

5 Contact Author Email Address

olivier.verseux@airbus.com
yannick.sommerer@airbus.com

Copyright Statement